

# Progress of ambient-pressure superconductivity in bilayer nickelate thin films

Wenyuan Qiu<sup>1</sup> and Dao-Xin Yao<sup>1,\*</sup>

<sup>1</sup>*Guangdong Provincial Key Laboratory of Magnetoelectric Physics and Devices,  
State Key Laboratory of Optoelectronic Materials and Technologies,  
School of Physics, Sun Yat-Sen University, Guangzhou, 510275, China*

This review summarizes recent progress of ambient-pressure superconductivity in bilayer nickelate  $\text{La}_3\text{Ni}_2\text{O}_7$  thin films, a major advancement following the discovery of high-pressure superconductivity in bulk  $\text{La}_3\text{Ni}_2\text{O}_7$ . First, we explain how epitaxial strain engineering enables ambient-pressure superconductivity in  $\text{La}_3\text{Ni}_2\text{O}_7$  thin films, with compressive strain from substrates like  $\text{SrLaAlO}_4$  stabilizing superconductivity. Next, we review experimental characterizations of related systems, with particular emphasis on ARPES measurements that have shown conflicting Fermi surface topologies. We then discuss progress in increasing the superconducting transition temperature  $T_c$ . Finally, we summarize theoretical studies of the electronic structure and pairing symmetry of  $\text{La}_3\text{Ni}_2\text{O}_7$  thin films. Together, these advances establish bilayer nickelate thin films as a highly tunable and promising platform for exploring high- $T_c$  superconductivity.

## INTRODUCTION

Since the discovery of superconductivity (SC) in copper oxides with a transition temperature ( $T_c$ ) of up to 164 K [1, 2], many efforts have been devoted to finding more high- $T_c$  superconductors. One of the promising candidates predicted to be a high- $T_c$  superconductor is nickel oxides, as nickel is located next to copper in the periodic table and is therefore believed to possess similar properties [3]. In 2019, the prediction was finally confirmed with the discovery of SC in an infinite-layer nickelate [4]. In 2023, Sun *et al.* [5] found SC with  $T_c$  near 80 K in bilayer nickelate  $\text{La}_3\text{Ni}_2\text{O}_7$  under high pressure, marking nickelates as the second class of high- $T_c$  superconductor to enter the liquid-nitrogen temperature range, following copper oxides. In 2024, Zhu *et al.* [6, 7] observed SC with  $T_c=20\text{-}30$  K under high pressure in trilayer nickelate  $\text{La}_4\text{Ni}_3\text{O}_{10}$ , further expanding the family of nickelate superconductors. However, the requirement of high pressure has significantly limited the use of specific key experimental techniques for directly investigating the superconducting phase. Consequently, considerable research has focused on achieving ambient-pressure SC in nickelates.

Recently, using pulsed laser deposition (PLD), Ko *et al.* [8] reported ambient-pressure SC with a  $T_c$  exceeding 40 K in  $\text{La}_3\text{Ni}_2\text{O}_7$  thin films grown on  $\text{SrLaAlO}_4$  (SLAO) substrates. Almost simultaneously, Zhou *et al.* [9] independently observed ambient-pressure SC with a  $T_c$  over 40 K in  $\text{La}_{2.85}\text{Pr}_{0.15}\text{Ni}_2\text{O}_7$  thin films grown on the same substrates by gigantic-oxidative atomic-layer-by-layer epitaxy (GAE). The microscopic structures of these thin films are shown in Fig. 1. Later, several groups reported ambient-pressure SC in related systems, including  $\text{La}_2\text{PrNi}_2\text{O}_7$  [10, 11], and  $\text{La}_{3-x}\text{Sr}_x\text{Ni}_2\text{O}_7$  thin films [12, 13]. These findings represent a significant advancement in the field of nickelate superconductors.

In this review, we begin by examining the role of epitaxial strain in enabling ambient-pressure SC in

$\text{La}_3\text{Ni}_2\text{O}_7$  thin films. We then examine key experimental studies, especially ARPES measurements that reveal distinct Fermi surface (FS) topologies, and summarize methods for raising the superconducting transition temperature  $T_c$ . Finally, we review recent theoretical studies of the electronic structures and possible pairing symmetry in  $\text{La}_3\text{Ni}_2\text{O}_7$  thin films.

## EFFECTS OF EPITAXIAL STRAIN

To achieve ambient-pressure SC, one promising approach is to apply epitaxial strain to  $\text{La}_3\text{Ni}_2\text{O}_7$  thin films. Before discussing the effects of epitaxial strain, it is necessary to analyze the pressure phase diagram of bulk  $\text{La}_3\text{Ni}_2\text{O}_7$  [16], which can be divided into a low-pressure region (LP) and a high-pressure region (HP). The characteristic structure of  $\text{La}_3\text{Ni}_2\text{O}_7$  is its bilayer  $\text{NiO}_2$  planes, where each layer contains a  $\text{NiO}_6$  octahedron [17, 18]. The two octahedra share an apical oxygen, forming a Ni-O-Ni bond. In the LP phase, the space group is  $Aman$ , characterized by a  $168^\circ$  bond angle. As the pressure approaches approximately 10 GPa, it transitions into the HP phase, characterized by two octahedra aligned with each other, leading to a bond angle tilting to  $180^\circ$  and

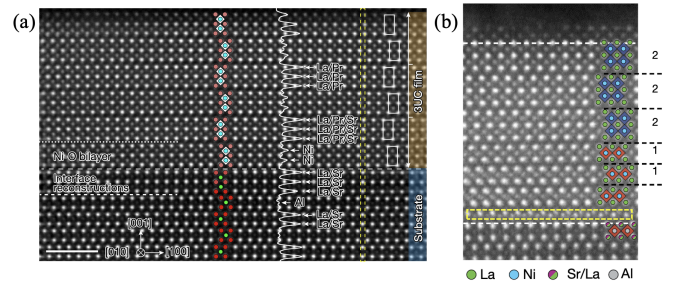


FIG. 1. Microscopic structures of (a)  $\text{La}_{2.85}\text{Pr}_{0.15}\text{Ni}_2\text{O}_7$  sample on  $\text{SrLaAlO}_4$  [9] and (b) of  $\text{La}_3\text{Ni}_2\text{O}_7$  on  $\text{SrLaAlO}_4$  [8].

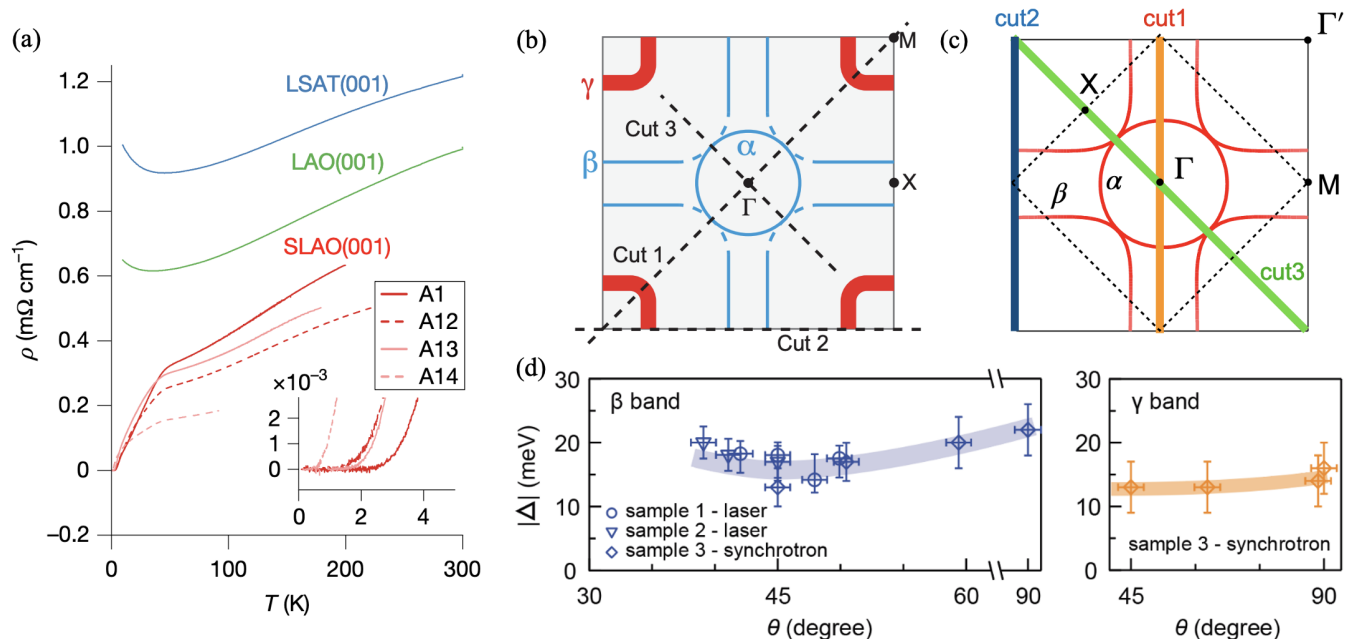


FIG. 2. (a) Temperature-dependent resistivity  $\rho(T)$  of  $\text{La}_3\text{Ni}_2\text{O}_7$  thin films grown on different substrates [8]. (b) FS of  $\text{La}_{2.85}\text{Pr}_{0.15}\text{Ni}_2\text{O}_7$  thin films, consisting of  $\alpha$ ,  $\beta$  and  $\gamma$  pockets [14]. (c) FS of  $\text{La}_2\text{PrNi}_2\text{O}_7$  thin films, without  $\gamma$  pocket appearing on FS [11]. (d) Measured superconducting gap magnitudes on the  $\beta$  and  $\gamma$  bands as a function of the angle  $\theta$  [15].

the space group changing to  $Fm\bar{3}m$  above 14 GPa and  $I4/m\bar{3}m$  above 46.8 GPa.

Since SC only appears in the HP phase, the main challenge is to stabilize this HP phase in thin films at ambient pressure. Cui *et al.* [19] revealed that epitaxial misfit strain is the dominant factor controlling the phase formation in RP nickelates  $\text{La}_{n+1}\text{Ni}_n\text{O}_{3n+1}$ . Their report indicates that tensile strain stabilizes the perovskite  $\text{LaNiO}_3$  ( $n=\infty$ ) phase, while compressive strain favors the formation of the  $\text{La}_3\text{Ni}_2\text{O}_7$  ( $n=2$ ) phase. Therefore, substrates play an important role in the induction of SC in bilayer nickelate thin films. As shown in Fig. 2 (a), the temperature-dependent resistivity  $\rho(T)$  of  $\text{La}_3\text{Ni}_2\text{O}_7$  thin films grown on SLAO substrates begins to decrease at approximately 42 K and reaches zero resistance near 2 K. In contrast,  $\rho(T)$  for films grown on  $\text{LaAlO}_3$  (LAO) and  $(\text{LaAlO}_3)_{0.3}(\text{Sr}_2\text{TaAlO}_6)_{0.7}$  (LSAT) substrates shows an upturn below 40 K without reaching a zero-resistance state [8]. The main difference among these substrates comes from their in-plane lattice constants, with SLAO applying compressive strain, LAO exerting only a mild compressive strain, and LSAT introducing a slight tensile strain. These results demonstrate that compressive strain is crucial for inducing ambient-pressure SC in  $\text{La}_3\text{Ni}_2\text{O}_7$  thin films. In addition, the results from Chen's group showed that the transition to zero resistance exhibits signatures of a Berezinskii-Kosterlitz-Thouless (BKT) transition [9].

## CHARACTERIZATION RESULTS

The absence of high-pressure requirements in these thin films enables direct experimental investigation of the superconducting phase. Consequently, various measurements have been performed on bilayer nickelate thin films to investigate the underlying mechanisms of SC. X-ray absorption spectroscopy (XAS) and scanning transmission electron microscopy (STEM) measurements show that Ni ions in the thin films maintain a mixed valence state, and the apical Ni-O-Ni bond angle approaches  $180^\circ$  [8], which is very similar to the HP phase of bulk  $\text{La}_3\text{Ni}_2\text{O}_7$ . Angle-resolved photoemission spectroscopy (ARPES) studies [11, 14, 15] on bilayer nickelate thin films have been conducted to confirm the topology of FS. As shown in Fig. 2 (b), ARPES measurements on  $\text{La}_{2.85}\text{Pr}_{0.15}\text{Ni}_2\text{O}_7$  thin films [14] reveal a FS, where the  $\alpha$ ,  $\beta$  and  $\gamma$  pockets are identified. Furthermore, direct measurement of the superconducting gap on the FS [15] reveals a significant gap opening on the  $\beta$  FS sheet with no signs of nodes along the Brillouin-zone diagonal, as shown in Fig. 2 (d). However, ARPES measurements on  $\text{La}_2\text{PrNi}_2\text{O}_7$  thin films [11] give a FS without the  $\gamma$  pocket, which is about 70 meV below the Fermi level, as shown in Fig. 2 (c). The contrast results may arise from differences in the growth conditions of the thin films. Scanning tunneling microscopy (STM) measurements [20] reveal a two-gap structure on the FS, with fitting analyses indicating a preferred anisotropic  $s$ -wave pairing. Taken together, these observations support a

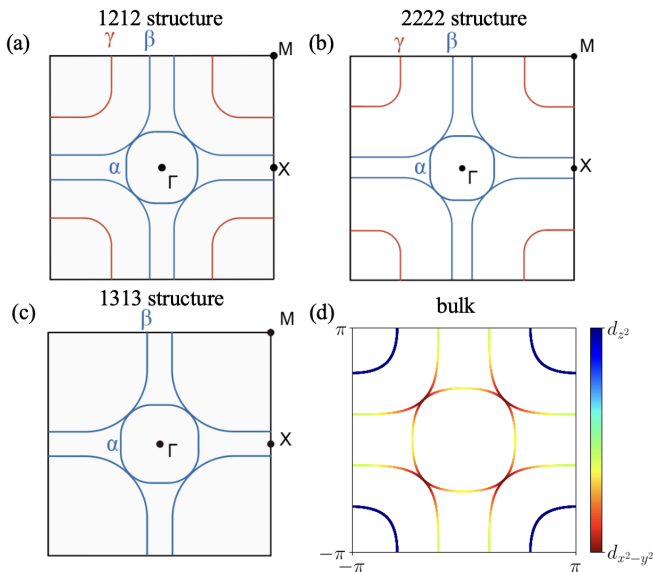


FIG. 3. FS [21] of thin films grown on SLAO substrates measured by ARPES for (a) 1212 structure, (b) 2222 structure, (c) 1313 structure and (d) bulk  $\text{La}_3\text{Ni}_2\text{O}_7$ .

predominant  $s\pm$ -wave pairing symmetry in the system. But whether the pairing symmetry is  $s\pm$  wave is still under debate. Most recently, Nie *et al.* [21] reported ambient-pressure SC with onset  $T_c$  up to 50 K in both hybrid monolayer-bilayer (1212) and pure bilayer (2222) films, while the hybrid monolayer-trilayer (1313) structure remained non-superconducting. The FS of these films measured by ARPES in Fig. 3 showed a clear difference: a hole-like  $\gamma$  band crosses the Fermi level in the superconducting films, but in the non-superconducting 1313 film, it is below the Fermi level, directly linking the FS topology to the presence of SC.

#### METHODS TO INCREASE $T_c$

Following the discovery of SC in bulk and thin-film  $\text{La}_3\text{Ni}_2\text{O}_7$ , methods to raise  $T_c$  have emerged as a major research focus. In thin film systems, methods to increase  $T_c$  mainly involve applying compressive strain and enhancing thin film growth techniques. Osada *et al.* [22] showed that as the  $c/a$  ratio increases, the onset  $T_c$  rises from approximately 10 K under tensile strain to nearly 60 K under compressive strain. Zhou *et al.* [23] showed that their improved GAE technique, achieved by pushing the growth regime into an extreme non-equilibrium state, can stabilize an ambient-pressure superconducting phase with an onset temperature of up to 63 K. Applying hydrostatic pressure on  $\text{La}_3\text{Ni}_2\text{O}_7$  thin films to compress the out-of-plane constant, which raises the onset  $T_c$  from 30 K to over 48 K, has also been reported recently [24]. And theoretical works [25, 26] have explored methods to en-

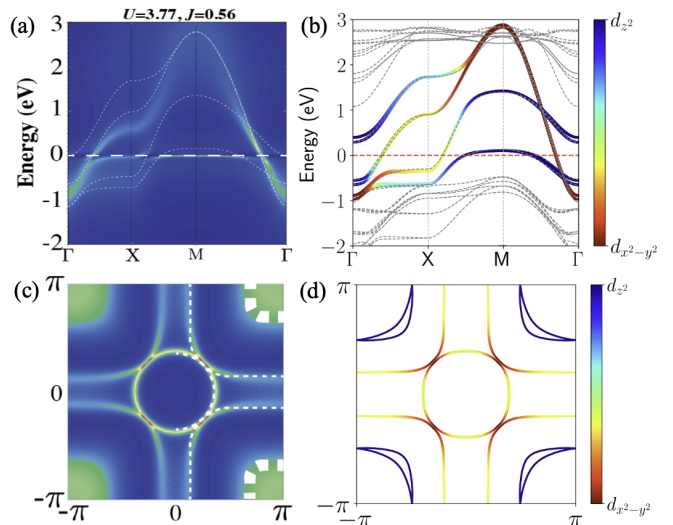


FIG. 4. (a) The energy bands and (c) FS of  $\text{La}_3\text{Ni}_2\text{O}_7$  thin films, combining DFT and DMFT [30]. (b) The energy bands and (d) FS of the One-UC double-stack tight-binding model for  $\text{La}_3\text{Ni}_2\text{O}_7$  thin films [31].

hance  $T_c$  by applying an electric field to thin films, which require experimental verification. While in bulk systems, using element substitution to increase  $T_c$  has advanced significantly. In bulk systems, Li *et al.* [27] reported bulk SC in  $\text{La}_2\text{SmNi}_2\text{O}_7$  under high pressure, which exhibits a  $T_c$  up to 96 K, zero resistance temperature up to 73 K, and clear Meissner screening, confirming robust bulk high- $T_c$  behavior. Qiu *et al.* [28] demonstrated that Nd substitution in bilayer  $\text{La}_3\text{Ni}_2\text{O}_7$  compresses the lattice and enhances interlayer magnetic coupling, resulting in SC with an onset  $T_c$  of up to approximately 93 K. Chen *et al.* [29] systematically calculated the electronic structures of Nd-doping bulk  $\text{La}_3\text{Ni}_2\text{O}_7$ , revealing that increasing Nd doping leads to a larger interlayer  $d_{z^2}$  orbital hopping, which would result in a larger interlayer superexchange coupling and a higher  $T_c$ .

#### THEORY PROGRESS OF BILAYER NICKELATE THIN FILMS

Since the discovery of SC in bilayer nickelate thin films, significant focus has been directed toward their underlying electronic structures. Several research groups subsequently performed systematic calculations of the electronic band structures [10, 30–34], employing first-principles density functional theory (DFT) and model analyses to characterize the low-energy states, FS topology, and orbital composition [35]. Using the constrained random phase approximation (cRPA), Yue *et al.* [30] demonstrated intra-orbital Coulomb interaction  $U \approx 3.77$  eV and Hund's coupling  $J_H \approx 0.56$  eV. Combining DFT and dynamical mean-field theory (DMFT) with

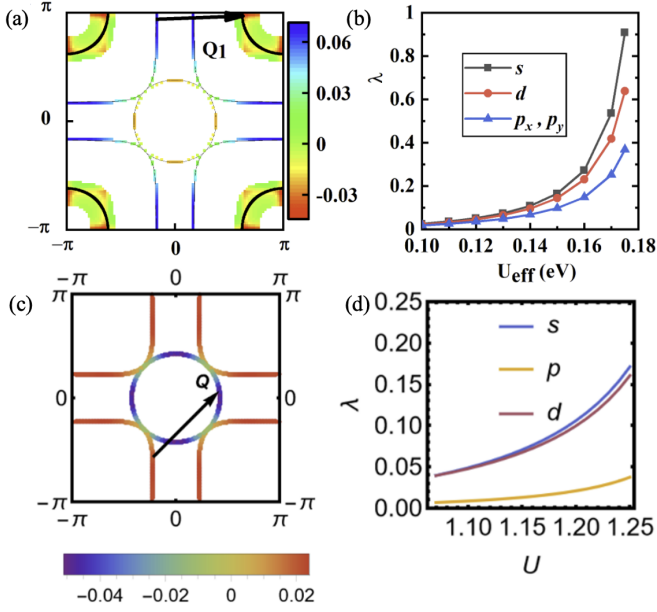


FIG. 5. (a) The leading cRPA calculated gap functions on the FS and (b) the dependence of  $\lambda$  on  $U_{eff}$  [30]. (c) The leading RPA calculated gap functions on the FS and (d) the dependence of  $\lambda$  on  $U$  without  $\gamma$  pocket [38].

the  $U$  and  $J_H$  obtained from cRPA and a particle filling of  $n = 1.3$ , they reproduced FS comparable to ARPES results, as shown in Fig. 4 (a) and (c). Using DFT, Hu *et al.* [31] systematically investigated the electronic structures and slab models across various thicknesses. They constructed the One-UC (unit cell) double-stack tight-binding model and the Half-UC slab model, which is used for comparison, and proposed a double-stack high-energy  $d$ - $p$  model for the first time, laying the groundwork for future research. The energy bands and FS of the One-UC double-stack tight-binding model are shown in Fig. 4 (b) and (d). Since the One-UC slab consists of two bilayers, there is some small hopping between the two bilayers, resulting in a small split of the  $\gamma$  pocket. It is notable that the interlayer  $d_{z^2}$  orbital hopping parameter for the One-UC slab is  $-0.550$ , while for the Half-UC slab it is  $-0.503$ . This suggests that the One-UC slab may have a larger interlayer  $d_{z^2}$  orbital superexchange coupling compared to the Half-UC case, according to  $J \sim 4t^2/U$ . Based on the double-stack model, the random phase approximation (RPA) spin susceptibility exhibits the strongest response reflecting nesting intra  $\gamma$  pocket. Building on a similar double-stack model, Li *et al.* [36] performed a DFT+ $U$  study of  $\text{La}_3\text{Ni}_2\text{O}_7/\text{SrLaAlO}_4$  thin films, explicitly incorporating both substrate-induced compressive strain and interfacial Sr interdiffusion. Recently, using DQMC and DMFT, Zhong *et al.* [37] reported that,  $\text{La}_3\text{Ni}_2\text{O}_7$  thin films exhibit a significantly enhanced charge-transfer capability together with interlayer and intralayer antiferromagnetic correlations of comparable magnitude.

Pairing symmetry is an important question in high- $T_c$  superconductors. Weak-coupling methods, such as RPA [40, 41] and functional renormalization group (FRG) [42, 43], are typically used to find out the pairing symmetry. Yue *et al.* [30] used a modified RPA approach based on their model, resulting in an  $s\pm$  wave pairing symmetry, as shown in Fig. 5 (a) and (b). However, the RPA approach is very sensitive to the details of FS. Shao *et al.* [38] constructed a tight-binding model without  $\gamma$  pocket, giving rise to an  $s\pm$  wave pairing symmetry, driven by nesting between the  $\alpha$  pocket and  $\beta$  pocket, as shown in Fig. 5 (c) and (d). Combining first-principles and FRG calculations, Le *et al.* [32] found that scattering between FS sheets with opposite parity symmetry enhances interlayer  $s\pm$  wave SC, while nesting between FS sheets with the same parity symmetry would break the pairing. Using FRG, Cao *et al.* [44] found that the pairing symmetry for both  $\text{La}_3\text{Ni}_2\text{O}_7$  and  $\text{La}_{2.85}\text{Pr}_{0.15}\text{Ni}_2\text{O}_7$  thin films is  $s\pm$  wave and  $T_c$  could be enhanced under in-plane compression. Recently, Zhang *et al.* [45] used the RPA approach on a one-UC compressive  $\text{La}_3\text{Ni}_2\text{O}_7$  thin film, revealing a leading  $d_{x^2-y^2}$  pairing state at moderate hole doping, and a  $d_{xy}$  pairing symmetry with higher doping level. Another theoretical method for identifying the pairing symmetry is the renormalized mean-field theory (RMFT) [46, 47], which begins with the  $t-J$  model. Qiu *et al.* [39] used the  $t-J$  Hamiltonian, including superexchange couplings  $J_{\perp}^z$ ,  $J_{\parallel}^x$ ,  $J_{xz}$ , and  $J_H$ , to investigate the pairing symmetry and superconducting gap structure on the FS in  $\text{La}_3\text{Ni}_2\text{O}_7$  thin films. Using exact diagonalization, the authors estimated  $J_{\perp}^z \approx 0.135$  eV. The resulting superconducting gap projected on the FS is shown in Fig. 6 (a), indicating a nodal  $s\pm$  wave pairing symmetry. The angular dependences of the gap on different pockets are shown in Fig. 6 (b)–(d). The gaps on the  $\beta$  and  $\gamma$  pockets are nodeless and have opposite signs, while a sign change occurs on the  $\alpha$  pocket. Whether there are nodes on the  $\alpha$  pocket still needs more experimental results to prove. On the  $\beta$  pocket, the gap shows a parabolic shape centered around  $45^\circ$ , and it slightly decreases as it nears the corner. Orbital-resolved superconducting gaps are displayed in Fig. 6 (e)–(h). Qiu *et al.* systematically studied the phase patterns and pointed out that they can be interpreted as maximizing the overall gap magnitude on FS [39]. As a result,  $\Delta_{\parallel}^z$  tends to maximize the gap on the  $\gamma$  pocket, whereas  $\Delta_{\parallel}^x$  enhances the gap on the  $\alpha$  pocket, with only minor suppression on the  $\beta$  pocket. Moreover, as temperature rises, the energy gap of all pairing bonds decreases to zero at approximately 60 K in a mean-field way, resulting in a  $T_c \approx 60$  K. Recently, some researchers have paid attention to the prediction of the  $T_c$  in superconductors [48, 49]. They tried to explore intrinsic constraints on the  $T_c$  in unconventional superconductors [48] and give an empirical scaling relation connecting the maximum  $T_c^*$  to the effective on-site Coulomb interaction  $U$  in unconventional

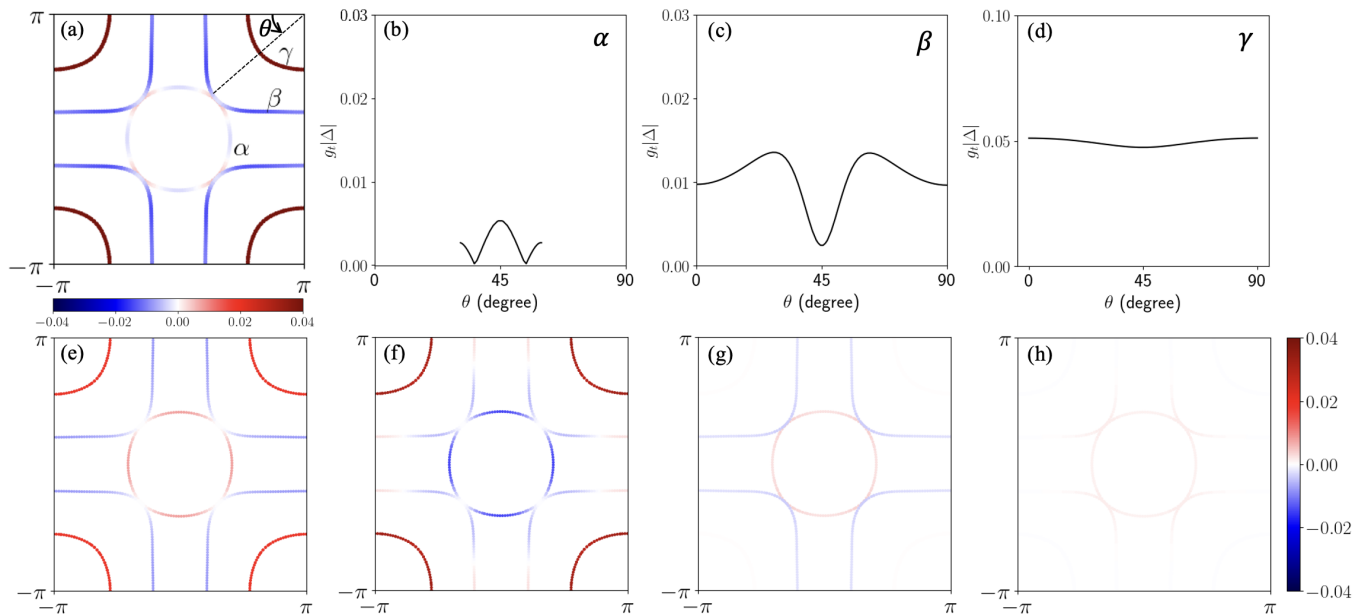


FIG. 6. (a) Superconducting gap projected on the FS and (b)-(d) superconducting gap as a function of angle for  $\alpha$ ,  $\beta$  and  $\gamma$  pockets, respectively. (e)-(h) Orbital-resolved superconducting gap on the FS for interlayer  $d_{z^2}$ , inplane  $d_{z^2}$ , interlayer  $d_{x^2-y^2}$  and inplane  $d_{x^2-y^2}$  pairing, respectively [39].

superconductors [49]. While the relation appears robust across some correlated superconductors, its microscopic origin remains an open question.

## SUMMARY

To date, some issues still need clarification. First, the role of the  $\gamma$  pocket in enabling SC in bilayer nickelate thin films remains to be fully clarified. Second, the relationship between the lattice ratio  $c/a$  and the superconducting transition temperature  $T_c$  in thin films differs from that in bulk  $\text{La}_3\text{Ni}_2\text{O}_7$ . These unresolved and seemingly contradictory results highlight the need for further experimental work to better understand SC in bilayer nickelate thin films.

## ACKNOWLEDGMENTS

We are grateful to Zihui Luo and Cui-Qun Chen for useful discussions. Work at Sun Yat-Sen University was supported by the National Natural Science Foundation of China (Grant Nos. 12494591, 92565303), the National Key Research and Development Program of China (Grant No. 2022YFA1402802), the Guangdong Provincial Key Laboratory of Magnetoelectric Physics and Devices (2022B1212010008), the Research Center for Magnetoelectric Physics of Guangdong Province (2024B0303390001), and the Guangdong Provincial Quantum Science Strategic Initiative (Grant

No. GDZX2401010).

\* yaodaax@mail.sysu.edu.cn

- [1] J. G. Bednorz and K. A. Müller, Possible high  $t_c$  superconductivity in the Ba-La-Cu-O system, *Zeitschrift für Physik B Condensed Matter* **64**, 189 (1986).
- [2] L. Gao, Y. Y. Xue, F. Chen, Q. Xiong, R. L. Meng, D. Ramirez, C. W. Chu, J. H. Eggert, and H. K. Mao, Superconductivity up to 164 k in  $\text{hgba}_2\text{cam-1cunO}_{2m+2+\delta}$  ( $m=1, 2$ , and  $3$ ) under quasihydrostatic pressures, *Phys. Rev. B* **50**, 4260 (1994).
- [3] V. I. Anisimov, D. Bukhvalov, and T. M. Rice, Electronic structure of possible nickelate analogs to the cuprates, *Phys. Rev. B* **59**, 7901 (1999).
- [4] D. Li, K. Lee, B. Y. Wang, M. Osada, S. Crossley, H. R. Lee, Y. Cui, Y. Hikita, and H. Y. Hwang, Superconductivity in an infinite-layer nickelate, *Nature* **572**, 624 (2019).
- [5] H. Sun, M. Huo, X. Hu, J. Li, Z. Liu, Y. Han, L. Tang, Z. Mao, P. Yang, B. Wang, J. Cheng, D.-X. Yao, G.-M. Zhang, and M. Wang, Signatures of superconductivity near 80 k in a nickelate under high pressure, *Nature* **621**, 493 (2023).
- [6] Y. Zhu, D. Peng, E. Zhang, B. Pan, X. Chen, L. Chen, H. Ren, F. Liu, Y. Hao, N. Li, Z. Xing, F. Lan, J. Han, J. Wang, D. Jia, H. Wo, Y. Gu, Y. Gu, L. Ji, W. Wang, H. Gou, Y. Shen, T. Ying, X. Chen, W. Yang, H. Cao, C. Zheng, Q. Zeng, J.-g. Guo, and J. Zhao, Superconductivity in pressurized trilayer  $\text{La}_4\text{Ni}_3\text{O}_{10-\delta}$  single crystals, *Nature* **631**, 531 (2024).
- [7] Q. Li, Y.-J. Zhang, Z.-N. Xiang, Y. Zhang, X. Zhu, and H.-H. Wen, Signature of superconductivity in pressurized

- $\text{La}_4\text{Ni}_3\text{O}_{10}$ , *Chin. Phys. Lett.* **41** (2024).
- [8] E. K. Ko, Y. Yu, Y. Liu, L. Bhatt, J. Li, V. Thampy, C.-T. Kuo, B. Y. Wang, Y. Lee, K. Lee, J.-S. Lee, B. H. Goodge, D. A. Muller, and H. Y. Hwang, Signatures of ambient pressure superconductivity in thin film  $\text{La}_3\text{Ni}_2\text{O}_7$ , *Nature* **638**, 935 (2025).
- [9] G. Zhou, W. Lv, H. Wang, Z. Nie, Y. Chen, Y. Li, H. Huang, W. Chen, Y. Sun, Q.-K. Xue, and Z. Chen, Ambient-pressure superconductivity onset above 40 K in  $(\text{La,Pr})_3\text{Ni}_2\text{O}_7$  films, *Nature* **640**, 641 (2025).
- [10] Y. Liu, E. K. Ko, Y. Tarn, L. Bhatt, J. Li, V. Thampy, B. H. Goodge, D. A. Muller, S. Raghu, Y. Yu, and H. Y. Hwang, Superconductivity and normal-state transport in compressively strained  $\text{La}_2\text{PrNi}_2\text{O}_7$  thin films, *Nature Materials*, 1 (2025).
- [11] B. Y. Wang, Y. Zhong, S. Abadi, Y. Liu, Y. Yu, X. Zhang, Y.-M. Wu, R. Wang, J. Li, Y. Tarn, E. K. Ko, V. Thampy, M. Hashimoto, D. Lu, Y. S. Lee, T. P. Devereaux, C. Jia, H. Y. Hwang, and Z.-X. Shen, Electronic structure of compressively strained thin film  $\text{La}_2\text{PrNi}_2\text{O}_7$  (2025), [arXiv:2504.16372](https://arxiv.org/abs/2504.16372).
- [12] B. Hao, M. Wang, W. Sun, Y. Yang, Z. Mao, S. Yan, H. Sun, H. Zhang, L. Han, Z. Gu, J. Zhou, D. Ji, and Y. Nie, Superconductivity and phase diagram in sr-doped  $\text{La}_{3-x}\text{Sr}_x\text{Ni}_2\text{O}_7$  thin films (2025), [arXiv:2505.12603](https://arxiv.org/abs/2505.12603).
- [13] H. Zhong, B. Hao, A. Chen, X. Huang, C. Li, W. Zhang, C. Liu, K. Kummer, N. Brookes, Y. Nie, T. Schmitt, and X. Lu, Doping evolution of spin excitations in  $\text{La}_{3-x}\text{Sr}_x\text{Ni}_2\text{O}_7/\text{SrLaAlO}_4$  superconducting thin films (2026), [arXiv:2603.01120](https://arxiv.org/abs/2603.01120).
- [14] P. Li, G. Zhou, W. Lv, Y. Li, C. Yue, H. Huang, L. Xu, J. Shen, Y. Miao, W. Song, Z. Nie, Y. Chen, H. Wang, W. Chen, Y. Huang, Z.-H. Chen, T. Qian, J. Lin, J. He, Y.-J. Sun, Z. Chen, and Q.-K. Xue, Angle-resolved photoemission spectroscopy of superconducting  $(\text{La, Pr})_3\text{Ni}_2\text{O}_7/\text{SrLaAlO}_4$  heterostructures, *Natl. Sci. Rev.* **12**, nwaf205 (2025).
- [15] J. Shen, G. Zhou, Y. Miao, P. Li, Z. Ou, Y. Chen, Z. Wang, R. Luan, H. Sun, Z. Feng, X. Yong, Y. Li, L. Xu, W. Lv, Z. Nie, H. Wang, H. Huang, Y.-J. Sun, Q.-K. Xue, J. He, and Z. Chen, Nodeless superconducting gap and electron-boson coupling in  $(\text{La,Pr,Sm})_3\text{Ni}_2\text{O}_7$  films (2025), [arXiv:2502.17831](https://arxiv.org/abs/2502.17831).
- [16] J. Li, D. Peng, P. Ma, H. Zhang, Z. Xing, X. Huang, C. Huang, M. Huo, D. Hu, Z. Dong, X. Chen, T. Xie, H. Dong, H. Sun, Q. Zeng, H.-k. Mao, and M. Wang, Identification of superconductivity in bilayer nickelate  $\text{La}_3\text{Ni}_2\text{O}_7$  under high pressure up to 100 GPa, *Natl. Sci. Rev.* (2025).
- [17] M. Wang, H.-H. Wen, T. Wu, D.-X. Yao, and T. Xiang, Normal and superconducting properties of  $\text{La}_3\text{Ni}_2\text{O}_7$ , *Chinese Physics Letters* **41**, 077402 (2024).
- [18] Y. Wang, K. Jiang, J. Ying, T. Wu, J. Cheng, J. Hu, and X. Chen, Recent progress in nickelate superconductors, *Natl. Sci. Rev.* **12**, nwaf373 (2025).
- [19] T. Cui, S. Choi, T. Lin, C. Liu, G. Wang, N. Wang, S. Chen, H. Hong, D. Rong, Q. Wang, *et al.*, Strain-mediated phase crossover in ruddlesden–popper nickelates, *Commun. Mater.* **5**, 32 (2024).
- [20] S. Fan, M. Ou, M. Scholten, Q. Li, Z. Shang, Y. Wang, J. Xu, H. Yang, I. M. Eremin, and H.-H. Wen, Superconducting gap structure and bosonic mode in  $\text{La}_2\text{PrNi}_2\text{O}_7$  thin films at ambient pressure (2025), [arXiv:2506.01788](https://arxiv.org/abs/2506.01788).
- [21] Z. Nie, Y. Li, W. Lv, L. Xu, Z. Jiang, P. Fu, G. Zhou, W. Song, Y. Chen, H. Wang, H. Huang, J. Lin, D. Shen, P. Li, Q.-K. Xue, and Z. Chen, Ambient-pressure superconductivity and electronic structures of engineered hybrid nickelate films (2025), [arXiv:2509.03502](https://arxiv.org/abs/2509.03502).
- [22] M. Osada, C. Terakura, A. Kikkawa, M. Nakajima, H.-Y. Chen, Y. Nomura, Y. Tokura, and A. Tsukazaki, Strain-tuning for superconductivity in  $\text{La}_3\text{Ni}_2\text{O}_7$  thin films, *Commun. Phys.* **8**, 251 (2025).
- [23] G. Zhou, H. Wang, H. Huang, Y. Chen, F. Peng, W. Lv, Z. Nie, W. Wang, Q.-K. Xue, and Z. Chen, Superconductivity onset above 60 K in ambient-pressure nickelate films, *Natl. Sci. Rev.*, nwag151 (2026).
- [24] Q. Li, J. Sun, S. Boetzel, M. Ou, Z.-N. Xiang, F. Lechermann, B. Wang, Y. Wang, Y.-J. Zhang, J. Cheng, I. M. Eremin, and H.-H. Wen, Enhanced superconductivity in the compressively strained bilayer nickelate thin films by pressure (2025), [arXiv:2507.10399](https://arxiv.org/abs/2507.10399).
- [25] Z.-Y. Shao, J.-H. Ji, C. Wu, D.-X. Yao, and F. Yang, Possible liquid-nitrogen-temperature superconductivity driven by perpendicular electric field in the single-bilayer film of  $\text{La}_3\text{Ni}_2\text{O}_7$  at ambient pressure, *Nat. Commun.* **17**, 10.1038/s41467-025-67880-5 (2026).
- [26] Z.-D. Fan and A. Vishwanath, Minimal two band model and experimental proposals to distinguish pairing mechanisms of the high- $T_c$  superconductor  $\text{La}_3\text{Ni}_2\text{O}_7$  (2025), [arXiv:2512.05956](https://arxiv.org/abs/2512.05956).
- [27] F. Li, Z. Xing, D. Peng, J. Dou, N. Guo, L. Ma, Y. Zhang, L. Wang, J. Luo, J. Yang, *et al.*, Bulk superconductivity up to 96 K in pressurized nickelate single crystals, *Nature*, 1 (2025).
- [28] Z. Qiu, J. Chen, D. V. Semenov, Q. Zhong, D. Zhou, J. Li, P. Ma, X. Huang, M. Huo, T. Xie, X. Chen, H. kwang Mao, V. Struzhkin, H. Sun, and M. Wang, Interlayer coupling enhanced superconductivity near 100 k in  $\text{La}_{3-x}\text{Nd}_x\text{Ni}_2\text{O}_7$  (2025), [arXiv:2510.12359](https://arxiv.org/abs/2510.12359).
- [29] C.-Q. Chen, W. Qiu, Z. Luo, M. Wang, and D.-X. Yao, Electronic structures and superconductivity in nd-doped  $\text{La}_3\text{Ni}_2\text{O}_7$  (2025), [arXiv:2510.08194](https://arxiv.org/abs/2510.08194).
- [30] C. Yue, J.-J. Miao, H. Huang, Y. Hua, P. Li, Y. Li, G. Zhou, W. Lv, Q. Yang, F. Yang, H. Sun, Y.-J. Sun, J. Lin, Q.-K. Xue, Z. Chen, and W.-Q. Chen, Correlated electronic structures and unconventional superconductivity in bilayer nickelate heterostructures, *Natl. Sci. Rev.* **12**, nwaf253 (2025).
- [31] X. Hu, W. Qiu, C.-Q. Chen, Z. Luo, and D.-X. Yao, Electronic structures and multi-orbital models of  $\text{La}_3\text{Ni}_2\text{O}_7$  thin films at ambient pressure (2025), [arXiv:2503.17223](https://arxiv.org/abs/2503.17223).
- [32] C. Le, J. Zhan, X. Wu, and J. Hu, Opposite-mirror-parity scattering as the origin of superconductivity in strained bilayer nickelates (2025), [arXiv:2501.14665](https://arxiv.org/abs/2501.14665).
- [33] H. Shi, Z. Huo, G. Li, H. Ma, T. Cui, D.-X. Yao, and D. Duan, The effect of carrier doping and thickness on the electronic structures of  $\text{La}_3\text{Ni}_2\text{O}_7$  thin films (2025), [arXiv:2502.04255](https://arxiv.org/abs/2502.04255).
- [34] L. Bhatt, A. Y. Jiang, E. K. Ko, N. Schnitzer, G. A. Pan, D. F. Segedin, Y. Liu, Y. Yu, Y.-F. Zhao, E. A. Morales, C. M. Brooks, A. S. Botana, H. Y. Hwang, J. A. Mundy, D. A. Muller, and B. H. Goodge, Resolving structural origins for superconductivity in strain-engineered  $\text{La}_3\text{Ni}_2\text{O}_7$  thin films (2025), [arXiv:2501.08204](https://arxiv.org/abs/2501.08204).
- [35] Z. Luo, X. Hu, M. Wang, W. Wú, and D.-X. Yao, Bilayer two-orbital model of  $\text{La}_3\text{Ni}_2\text{O}_7$  under pressure, *Phys. Rev. Lett.* **131**, 126001 (2023).

- [36] G. Li, C.-Q. Chen, H. Shi, Z. Liu, H. Ma, F. Tian, D.-X. Yao, and D. Duan, Theoretical study on the electronic properties and multiorbital models of  $\text{La}_3\text{Ni}_2\text{O}_7$  thin films on  $\text{SrLaAlO}_4$  (001) (2025), [arXiv:2512.17625](#).
- [37] Y. Zhong, W. Wú, and D.-X. Yao, Superexchanges and charge transfer in the  $\text{La}_3\text{Ni}_2\text{O}_7$  thin films (2025), [arXiv:2511.04739](#).
- [38] Z.-Y. Shao, C. Lu, M. Liu, Y.-B. Liu, Z. Pan, C. Wu, and F. Yang, Pairing without  $\gamma$ -pocket in the  $\text{La}_3\text{Ni}_2\text{O}_7$  thin film (2025), [arXiv:2507.20287](#).
- [39] W. Qiu, Z. Luo, X. Hu, and D.-X. Yao, Pairing symmetry and superconductivity in  $\text{La}_3\text{Ni}_2\text{O}_7$  thin films (2025), [arXiv:2506.20727](#).
- [40] Y.-B. Liu, J.-W. Mei, F. Ye, W.-Q. Chen, and F. Yang, The  $s^\pm$ -wave pairing and the destructive role of apical-oxygen deficiencies in  $\text{La}_3\text{Ni}_2\text{O}_7$  under pressure, *Phys. Rev. Lett.* **131** (2023).
- [41] Y. Zhang, L.-F. Lin, A. Moreo, T. A. Maier, and E. Dagotto, Structural phase transition,  $s^\pm$ -wave pairing, and magnetic stripe order in bilayered superconductor  $\text{La}_3\text{Ni}_2\text{O}_7$  under pressure, *Nat. Commun.* **15**, 2470 (2024).
- [42] Q.-G. Yang, D. Wang, and Q.-H. Wang, Possible  $s_\pm$ -wave superconductivity in  $\text{La}_3\text{Ni}_2\text{O}_7$ , *Phys. Rev. B* **108**, L140505 (2023).
- [43] K.-Y. Jiang, Y.-H. Cao, Q.-G. Yang, H.-Y. Lu, and Q.-H. Wang, Theory of pressure dependence of superconductivity in bilayer nickelate  $\text{La}_3\text{Ni}_2\text{O}_7$ , *Phys. Rev. Lett.* **134** (2025).
- [44] Y.-H. Cao, K.-Y. Jiang, H.-Y. Lu, D. Wang, and Q.-H. Wang, Strain-engineered electronic structure and superconductivity in  $\text{La}_3\text{Ni}_2\text{O}_7$  thin films, *Sci. China Phys. Mech. Astron.* **69**, 247412 (2026).
- [45] Y. Zhang, L.-F. Lin, A. Moreo, S. Okamoto, T. A. Maier, and E. Dagotto, Compressive strain turns  $s^\pm$  into  $d$ -wave pairing in one-unit-cell  $\text{La}_3\text{Ni}_2\text{O}_7$  thin film via substrate-induced hole doping (2025), [arXiv:2512.19520](#).
- [46] Z. Luo, B. Lv, M. Wang, W. Wú, and D.-X. Yao, High- $T_c$  superconductivity in  $\text{La}_3\text{Ni}_2\text{O}_7$  based on the bilayer two-orbital t-J model, *npj Quantum Mater.* **9**, 1 (2024).
- [47] F. C. Zhang, C. Gros, T. M. Rice, and H. Shiba, A renormalised Hamiltonian approach to a resonant valence bond wavefunction, *Supercond. Sci. Technol.* **1**, 36 (1988).
- [48] Q. Qin and Y.-f. Yang, Intrinsic constraint on  $T_c$  for unconventional superconductivity, *npj Quantum Materials* **10**, 13 (2025).
- [49] W. Wang, Z. Ma, and H. qing Lin, A universal scaling law for  $T_c$  in unconventional superconductors (2025), [arXiv:2510.25082](#).